ELSEVIER

Contents lists available at ScienceDirect

Quaternary Geochronology

journal homepage: www.elsevier.com/locate/quageo





Cosmogenic nuclide burial dating at Penhill Farm: An Earlier Stone Age Acheulean locality in the lower Sundays River Valley, South Africa

Matt G. Lotter^{a,*}, Kathleen Kuman^b, Darryl E. Granger^{c,**}

- ^a Palaeo-Research Institute. University of Johannesburg, P.O. Box 524, Auckland Park, 2006, South Africa
- b School of Geography, Archaeology and Environmental Studies, University of the Witwatersrand, Johannesburg, WITS 2050, South Africa
- ^c Department of Earth, Atmospheric and Planetary Sciences, Purdue University, IN, 47907, USA

ARTICLE INFO

Keywords: Acheulean techno-complex Cosmogenic nuclide burial dating Lithic assemblage Debris flow

ABSTRACT

Penhill Farm is an Earlier Stone Age (ESA) Acheulean archaeological site located within the southeastern Cape coastal region of South Africa. Although ESA artifacts have been known for this region since the 1950s, limited archaeological work and an inability to date the terrace context sites have prevented understanding the technological progression from the ESA to Middle Stone Age (MSA) and their placement within the Stone Age chronology of South Africa. Here we use cosmogenic ²⁶Al and ¹⁰Be to reveal a two-stage depositional history for a stone tool assemblage recovered from a debris flow deposit, with artifacts dating to ca. 1.1 Ma (million years) incorporated into a debris flow dating to ca. 0.6 Ma, thereby constraining the Penhill Farm Acheulean occupation to the Early Pleistocene.

1. Introduction

Fluvial terraces

The southern Cape coast of South Africa preserves an exceptional array of Middle Stone Age/Middle Palaeolithic (MSA/MP) sites spanning the Middle to Late Pleistocene (with sites dating to between 166 and 45 thousand years). Collectively they illustrate the proliferation of Homo sapiens (Lombard et al., 2012; Wurz 2020), as evidenced by the types of recovered artifacts, some of which document the earliest forms of complex symbolism, abstract thought, and modernity (e.g., engraved objects and personal ornamentation, amongst others; Henshilwood et al., 2002; Henshilwood et al., 2004; Marean 2010; Wurz 2013). This region has a remarkable record that depicts a complex landscape where humans adapted to their coastal/near-coastal environments and took advantage of the local landscape. These sites have been fundamental in ameliorating our understanding of when our species became modern – a question of global significance – as reflected by a suite of characteristic behaviors and preserved material culture that indicates increased cognitive complexity (see discussions by McBrearty & Brooks [2000], d'Errico & Stringer [2011], and Wurz [2013]).

Less is known about earlier archaeological signatures along the southern Cape coast, particularly for the Eastern Cape Province where there has been a limited number of sites reported. This is not to say these

earlier signs of occupation are not present on the landscape, but rather that this region has suffered from investigative neglect. Earlier Stone Age (ESA) artifacts were first reported in this region by Laidler (1947) at Geelhoutboom, and subsequently in the Coega and Sundays River Valleys by Ruddock (1957). This was followed later by reports from perhaps the most well-known ESA site for the region, Amanzi Springs (Inskeep 1965; Deacon 1970; see Suppl. Fig. 1), and by subsequent coastal surveys by Davies (1971, 1972). While these earlier studies support regional occupation during the ESA, detailed understanding has been limited by the context of some of these sites (e.g., surface scatters) and by dating issues. In addition, over the past 50 years only a single ESA site has been excavated for this region. As a result, we have until recently been unable to situate stone-tool-making hominins on the regional landscape and to contextualize Early Pleistocene technological developments, in addition to being unable to clarify the period of transition during the ESA between the later Acheulean and the emergence of the MSA (that occurs between ca. >200 ka and ca. 500 ka - Lombard et al., 2012, Wilkins and Chazan 2012; for detailed discussions on this transition, see Kuman et al., 2020). This is important given that this landscape provides a unique coastal/near-coastal environment with highly variable vegetation, topography, climate and geology, all of which would have influenced the way hominins adapted to their

E-mail addresses: mattlotter@gmail.com (M.G. Lotter), dgranger@purdue.edu (D.E. Granger).

^{*} Corresponding author.

^{**} Corresponding author.

surroundings.

A new research program was initiated in 2016 to describe and date ESA sites in the lower Sundays River Valley (Fig. 1; Lotter 2016). This research was facilitated by an earlier geochronological study that applied cosmogenic nuclide burial dating to a series of preserved (relict) alluvial terraces in the lower part of the valley (Erlanger et al., 2012). The study provided a chronology for the terrace sequence and confirmed that ESA – and specifically Acheulean artifacts that had originally been reported several decades earlier by Ruddock (1957) – were preserved within the dated terraces. This subsequently led to excavations at three key terrace sites (Lotter and Kuman 2018a, b; Lotter, in press): namely Atmar Farm (0.65 \pm 0.12 Ma), Bernol Farm (1.14 \pm 0.12 Ma), and Penhill Farm for which we report new dating results here.

2. The Sundays River Valley terraces, dating, and Penhill Farm site description

The terraces of the Sundays River, preserved in the lower part of the valley that stretches from the Klein Winterhoek Mountains in the northwest to the river's outflow to the Indian Ocean in the southeast, were first recorded nearly a century ago by S.H. Haughton (1928). Since

their identification, numerous scholars have sought to explain their formation, preservation, age, composition, and significance (for debates on their evolution, see: Ruddock 1948, 1968; Hattingh 1994, 1996, 2008; Hattingh and Goedhart 1997; Dollar 1998; Hattingh and Rust 1999). These fluvial deposits reflect the interplay between the complex regional geology of the Algoa Basin and the near-coastal environment of the valley, recording changes in the drainage evolution of the river through time as the river incised into the highly erodible shales and mudstones of the Uitenhage Group (Ruddock 1948; Hattingh and Rust 1999; see Suppl. Fig. 1). The terrace deposits are composed primarily of gravels and fine silts and sands, extremely rich in quartzite and sandstone (>95% of clasts downstream) derived from the upstream Klein Winterhoek Mountains (Witteberg Group; see Suppl. Fig. 1; Ruddock 1948; Hattingh 1994; Hattingh and Rust 1999).

Hattingh and collaborators (Hattingh 1994, 1996, 2008; Hattingh and Goedhart 1997; Hattingh and Rust 1999) identified 13 terraces (Fig. 1b). These have been grouped into sets of higher and lower terraces, with the higher Terraces 1–9 (180-40 m above river level) formed on straths, and the lower Terraces 10–13 largely formed in a sedimentary fill inset into the valley floor (Fig. 1). At the time, these authors estimated the higher terraces to have formed during the Late Miocene

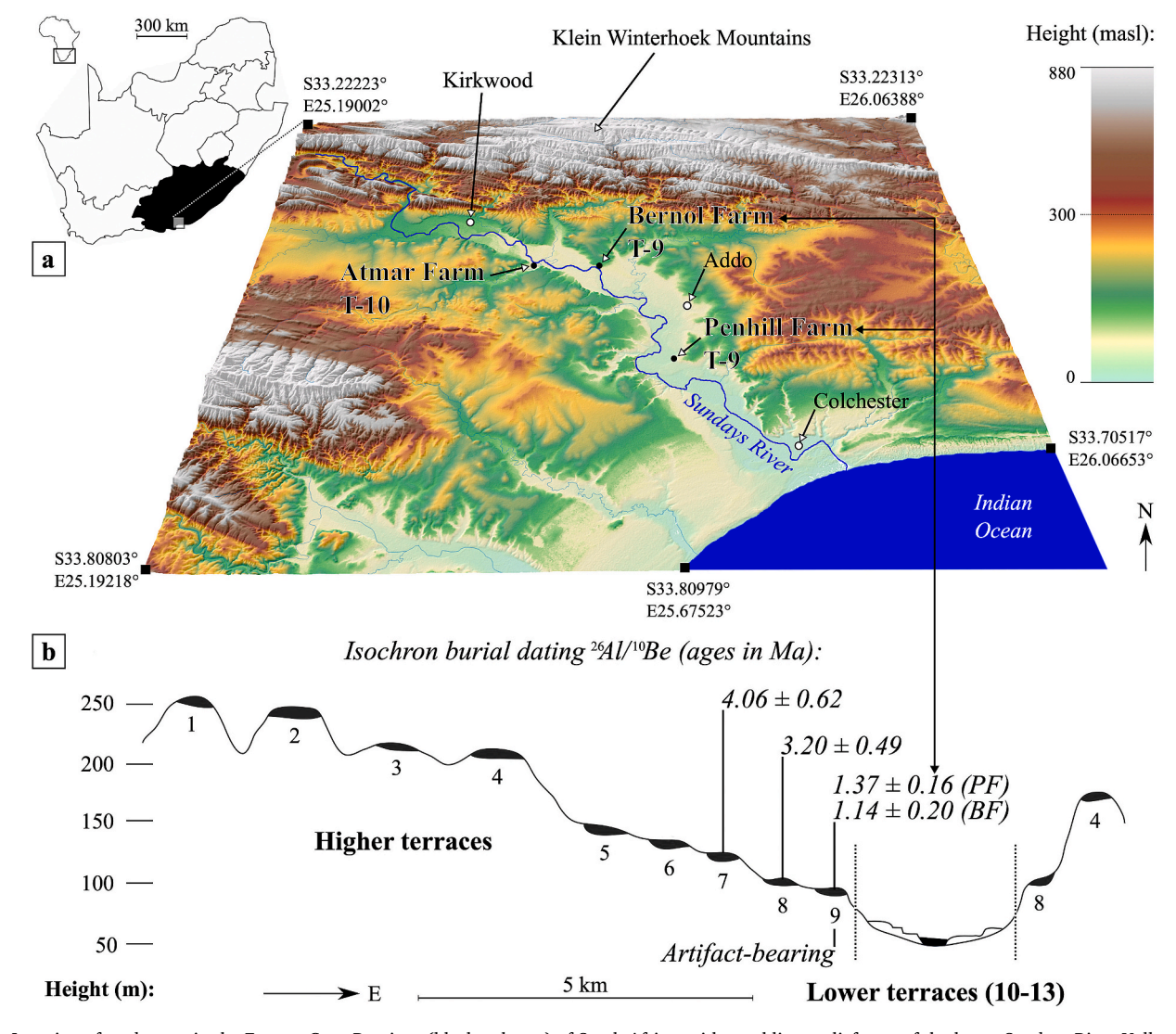


Fig. 1. Location of study area in the Eastern Cape Province (black polygon) of South Africa, with an oblique relief map of the lower Sundays River Valley and the surrounding landscape (a: mapping data obtained from CSIR 2011; NASA JPL 2013). Synthetic cross section showing fluvial terrace sequence (nine higher = Terrace 1 to 9; four lower = Terrace 10 to 13) with heights (b: redrawn and modified after Erlanger 2010; Hattingh 2008; modified from Lotter and Kuman 2018a) and ages (data from Erlanger et al., 2012; Granger et al., 2013).

through to the Pliocene, while the lower terraces formed in the Pleistocene and Holocene. Overall terrace capping sediment thicknesses range from 3 to 12 m (Hattingh 1996).

To investigate terrace ages and long-term river incision and uplift rates, Erlanger et al. (2012) applied cosmogenic ²⁶Al and ¹⁰Be isochron burial dating to gravels and sands and provided a radiometric chronology for Terraces 7–13. Most relevant for this study, at one of their Terrace 9 sampling locations at Penhill Farm, Erlanger et al. (2012) identified ESA artifacts eroding out from an exposed deposit.

Penhill Farm is a citrus producing establishment that preserves a vertical, semi-circular exposure of Terrace 9 alluvium in a borrow pit along its southern boundary, approximately 1.6 km from the present river and 20 km from the Indian Ocean (Fig. 2). The exposure comprises several meters of massive, structureless, fine and lightly colored overbank silts and sands (Fig. 2a and b). Imbricated pebbles and cobbles underlie the overbank fines, and it is from within the top meter of this gravel horizon that Erlanger et al. (2012) sampled gravels for cosmogenic nuclide isochron burial dating (Fig. 2c and d), over a vertical range of ca. 10 cm. They provided an age of 1.37 \pm 0.16 Ma for terrace deposition (as refined by Granger et al., 2013). Stone Age artifacts were noted by Erlanger et al. (2012) in a gravel stringer within the sands, but otherwise artifacts have not been found in the underlying gravels nor distributed in the overlying sands.

The observation of artifacts in the gravel stringer – an isolated gravel layer in the sand – prompted Lotter (2016) to conduct a 10 m² excavation to target the deposit, with the aims to clarify its formational history and obtain a sample of the artifacts to characterize their techno-typological characteristics (for descriptions of the Penhill Farm archaeology, see Lotter and Kuman 2018a; Lotter 2020a, b, 2022; Mesfin et al., 2021; Lotter and Caruana 2021; Caruana and Lotter 2022). The excavation revealed that the artifacts were in an eroded channel (gully) that cut into the surrounding alluvium (Fig. 3), also visible in profile in the vertical walls of the terrace exposure (Fig. 4a and b). The channel subsequently infilled with poorly sorted sandy colluvium, including pebble-sized clasts of terrace sand indurated to varying degrees by pedogenic calcite and silica. The basal channel fill contains a distinct debris flow facies that is discontinuous, 20–50 cm thick, and constrained to the base of the channel (what Erlanger et al., 2012 termed a gravel

stringer exposed in cross section). The debris flow deposit contains an extremely abundant collection of well-preserved ESA artifacts. It likely originated from a nearby source area upslope while sweeping a lag of calcrete and silcrete nodules, gravels and artifacts downslope to infill the base of the channel (Granger et al., 2013). Non-artifact-bearing overbank silts and sands occur directly under the flow, from a depth of approximately 2.5 m, and these continue downwards for several meters until (presumably) reaching the level of the underlying gravels like those to the south (Fig. 2c and d). The channel fill overlying the basal debris flow contains only sporadic artifacts, gravels, and calcrete and silcrete nodules.

The clasts in the artifact-bearing channel were likely derived from erosion of a higher gravel terrace exposed upslope at an elevation some 20-30 m higher than the Penhill terrace. Although raw materials for the artifacts could have been carried from the active riverbed, the nonartifactual clasts would almost certainly have been derived from uphill where gravels exposed on the terrace surface would have been readily available for stone tool production. This higher terrace was not dated directly, but it likely corresponds to Terrace 8 of Hattingh (1996), dated elsewhere by Erlanger et al. (2012) to 3.20 \pm 0.49 Ma (Fig. 1). An artifact-bearing colluvial wedge is developed on the flank of the upper terrace, and exposures in gullies show that it contains abundant quartz-bearing gravel as well as pedogenic calcrete and silcrete that was eroded from the soils upslope (Fig. 3). The gully floors contain concentrated deposits of the coarser gravels and pedogenic nodules. The toe of the wedge (where the accumulated colluvium meets the Terrace 9 surface) presently lies less than 30 m upslope from the excavation. We suggest that the Penhill Farm artifacts were originally sourced from the upper terrace surface, and that they then accumulated within the colluvial wedge. After remaining buried for some time in the colluvium, they were incorporated into a debris flow together with clasts of pedogenic calcrete and silcrete and carried to the excavation site.

The 1.37 \pm 0.16 Ma burial age of the Terrace 9 gravel (Erlanger et al., 2012) has previously served as a maximum for the Penhill Farm archaeology (Lotter and Kuman 2018a), because the burial age dates deposition of the terrace, which is necessarily older than the channel cut into it. To better constrain the artifacts themselves, we sampled gravel and artifacts directly from the debris flow layer in the excavation.

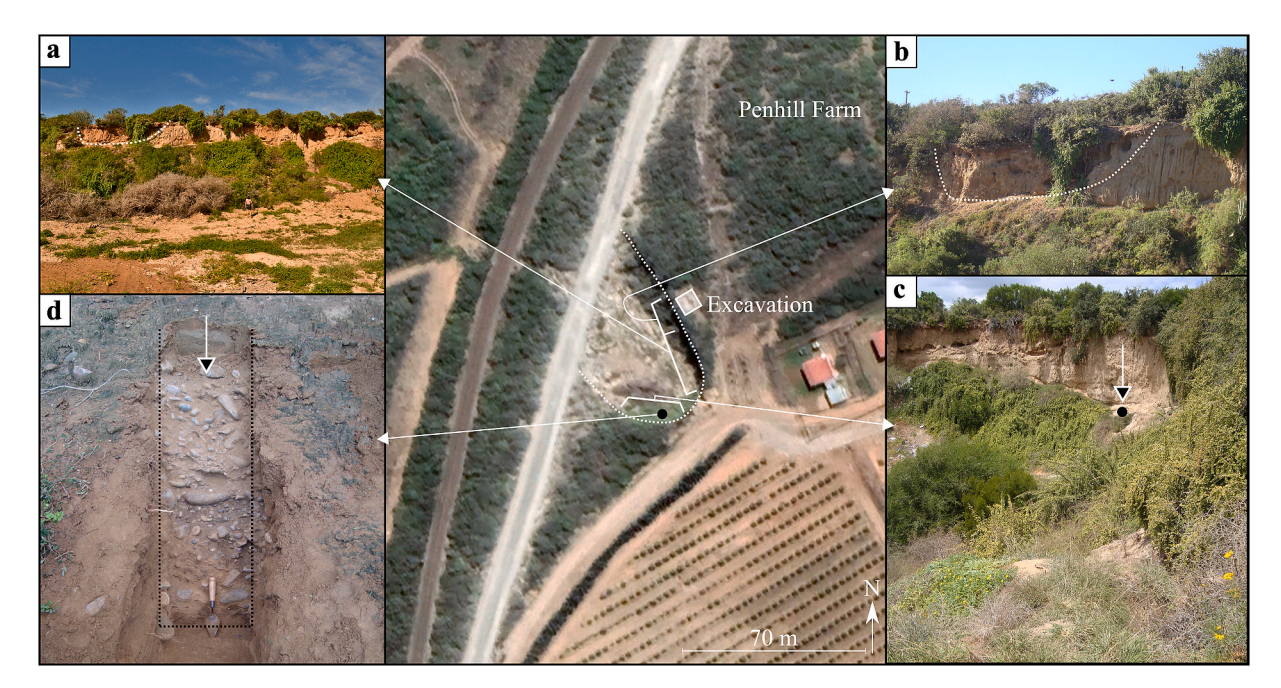


Fig. 2. Location of the Penhill Farm excavation (center image) with portions of the Terrace 9 exposure (stippled line = terrace edge) indicated by the inset images (a-d). North-eastern terrace exposure (a: note person right of center for scale) with the erosion channel visible (stippled line; see b for a closer view and see Fig. 4 for details of the erosion channel). Towards the south, the Erlanger et al. (2012) sampling location (c) and upper 1 m of the gravel deposit (d; note trowel for scale).

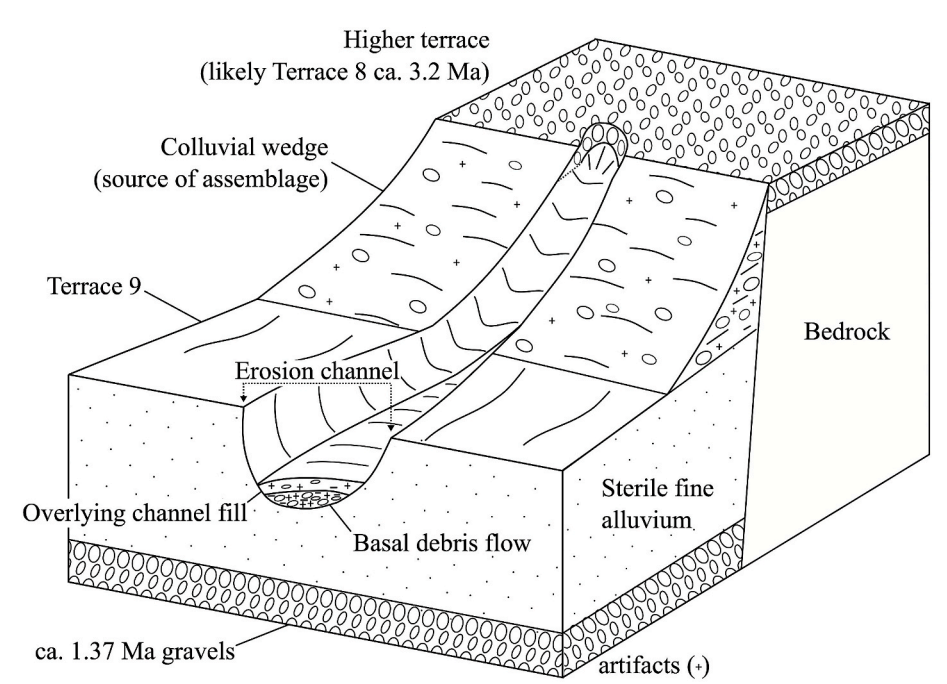


Fig. 3. Cartoon illustrating the geomorphic setting of the artifact-bearing deposit at Penhill Farm in relation to an older higher terrace upslope, which likely corresponds with Terrace 8. The artifacts are found concentrated in a debris flow deposit (deposit 2 in Fig. 4b) within a channel cut into sterile overbank sands (deposit 3 in Fig. 4b) of a previously dated lower terrace. The debris flow and artifacts are sourced from a nearby colluvial wedge that has accumulated along the riser to the higher gravel-capped terrace. The colluvial wedge occurs a short distance upslope from the excavation.

3. Methods

Samples to be dated were obtained from a central square in the excavated portion of the debris flow deposit at the base of the channel (Square DD1; Table 1; Fig. 4c). All samples were obtained from between 215 and 240 cm below datum, vertically within 25 cm of each other, all within the same 1×1 m square, and directly from within the debris flow with an average overburden of 2.09 m. Prior to removal, samples were spatially mapped using a Nikon NPL-302 total station. In total, 13 clasts were obtained, including nine naturally rounded to sub-angular pebbles and cobbles, all comprised of quartzite, and four quartzite stone tools (see Suppl. Fig. 2 for images of the samples). Where needed, masses (in grams) and lengths (in millimeters) were also recorded (Table 1). Permits (ref#: 10,059 and 6212) were obtained from the South African Heritage Resources Agency (SAHRA) to export the samples to the Purdue Rare Isotope Measurement Laboratory (PRIME), Department of Earth, Atmospheric and Planetary Sciences (Purdue University, IN, USA), for processing. One sample did not yield enough clean quartz for analysis and is not further reported.

To date the gravels, we use the cosmogenic nuclide isochron burial dating method (Erlanger et al., 2012), based on the radioactive decay of $^{26}\mathrm{Al}$ and $^{10}\mathrm{Be}$ in quartz. These two cosmogenic nuclides are produced by exposure to secondary cosmic radiation near the ground surface. Because the secondary cosmic rays are rapidly attenuated with depth, after the rocks are buried in the debris flow channel, the $^{26}\mathrm{Al}$ and $^{10}\mathrm{Be}$ inherited from prior exposure decays over time due to radioactivity. By determining the remaining $^{26}\mathrm{Al}$ and $^{10}\mathrm{Be}$ concentrations and accounting for any continued production after burial, the depositional time can be calculated. A detailed explanation of the methodology can be found in Granger (2014).

The standard approach for isochron burial dating is to assume that the sediment was only buried once, and that it was derived from a landscape eroding in steady-state. In that case, we can express the relationship between the concentrations of 26 Al and 10 Be as equation (1 below), where N_{26} and N_{10} represent the concentrations of 26 Al and 10 Be, P_{26} and P_{10} represent production rates in the source area prior to burial, t represents the burial age, τ_{26} and τ_{10} represent radioactive meanlives of 26 Al (1.02 \pm 0.08 Ma; Nishiizumi, 2004) and 10 Be (2.00 \pm 0.02 Ma; Chmeleff et al., 2010; Korschinek et al., 2010), τ_{bur} is an effective meanlife given by $\tau_{bur} = (\tau_{26}^{-1} - \tau_{10}^{-1})^{-1}$, and $N_{26,pb}$ and $N_{10,pb}$

represent the concentrations of $^{26}\mathrm{Al}$ and $^{10}\mathrm{Be}$ that accumulated post-burial.

$$N_{26} = \left(N_{10} - N_{10,pb}\right) \left[\frac{\frac{P_{26}}{P_{10}} e^{-t_{\gamma_{bur}}}}{1 + \frac{N_{10}}{P_{10}\tau_{10}} e^{t_{\gamma_{bur}}}} \right] + N_{26,pb}$$
 (1)

By collecting multiple samples at the same burial depth, we can assume that the post-burial cosmogenic nuclide concentrations are identical for all samples. The samples will plot as a gentle curve on a graph of ²⁶Al versus ¹⁰Be, with the slope controlled by the age. Solution of equation (1), however, requires additional constraints on the post-burial components. If we assume that the samples were buried rapidly and have remained at approximately their present depth, then the post-burial cosmogenic nuclide concentrations can be determined using equation (2 below) for both nuclides

$$N_{i,pb} = P_{i,pb} \tau_i \left(1 - e^{-t/\tau_i} \right)$$
 (2)

where the subscript i indicates either ²⁶Al or ¹⁰Be, and $P_{i,pb}$ is the production rate after burial. Solution of equations (1) and (2) does not require knowledge of the absolute post-burial production rates, but only the ratio $P_{26,pb}/P_{10,pb}$.

However, the assumptions in the standard isochron approach expressed in equation (1) do not apply at Penhill Farm. For this site, each of the quartz clasts was originally eroded from the Klein Winterhoek mountains, then deposited on the higher river terrace nearby, undated, but likely Terrace 8. The terrace then eroded over time, bringing buried clasts up to the surface where they were collected as raw materials or were transported onto the colluvial wedge. The clasts were then reburied in the colluvial wedge, and finally transported to the excavation site in a debris flow. The history of any individual clast, then, includes a history of transport and multiple burial episodes. We can nonetheless place some constraints on the timing of sediment deposition.

For Penhill Farm, we can construct a model in which sediment was buried twice: first for a time t_1 on an eroding terrace, and then for a time t_2 in the colluvial wedge and at the excavation site (the sum of the two times t_1+t_2 is equal to the age of the upper terrace). The concentration of 26 Al or 10 Be for a two-stage burial scenario such as this is given by

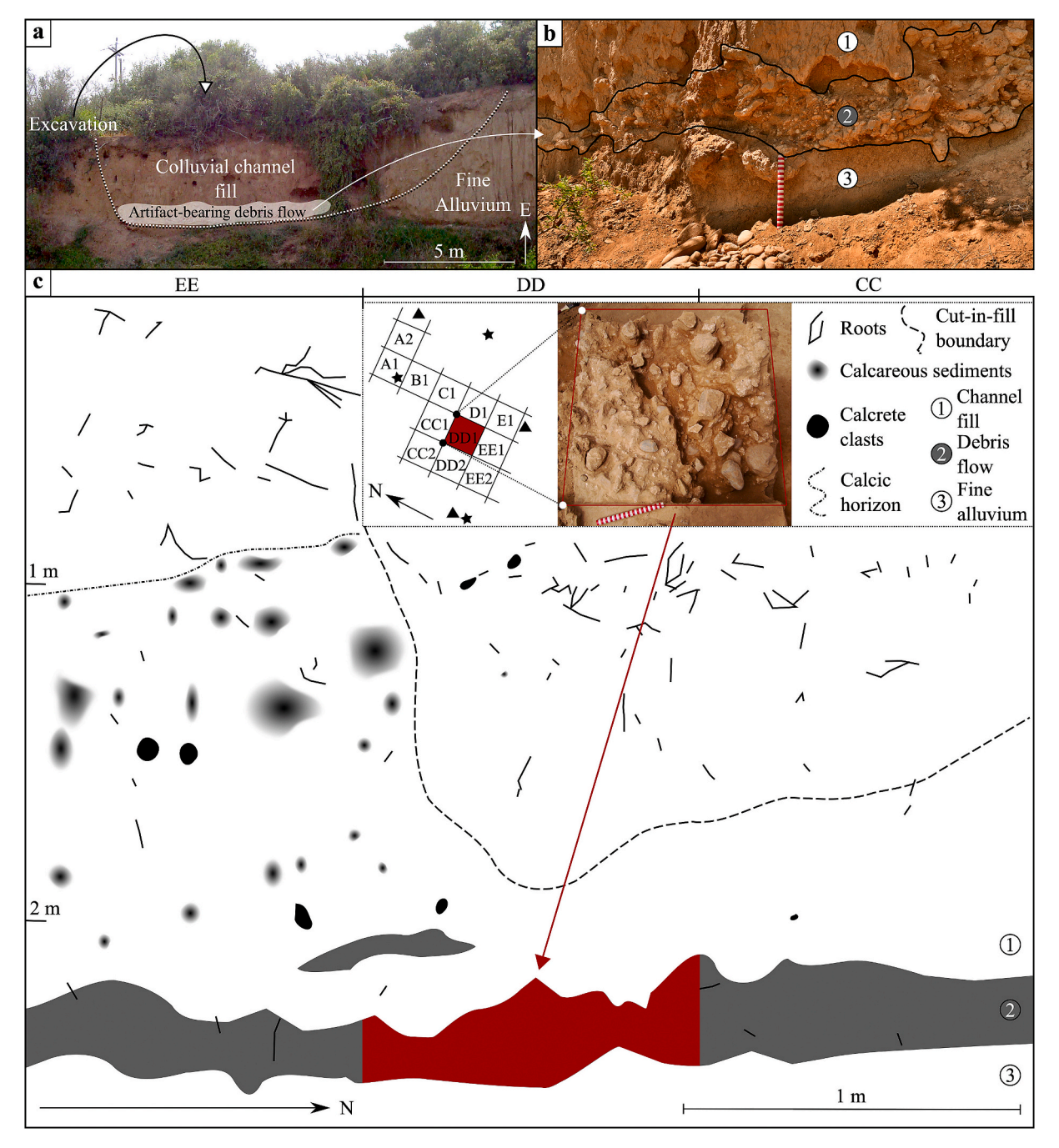


Fig. 4. Penhill Farm deposit exposure showing the debris flow, erosion channel (dashed line), and location of the excavation above and behind the exposure (a: modified from Lotter and Kuman 2018a). Close up of the exposure showing the local depositional sequence (b: scale is 30 cm; modified from Mesfin et al., 2021). West wall excavation profile with dated portion of the debris flow highlighted (c: with inset images shown in an unmapped section of the profile; modified from Lotter, in press). The inset comprises three components: left image, plan view of the excavation (dating sample square also highlighted; stars = mapping datums; triangles = line level datums); middle image, plan view of the exposed surface of the debris flow in the sampling square prior to excavation; right image, profile key.

equation (3), where ρ is density, E is the erosion rate of the terrace, and Λ is the penetration length of the secondary cosmic rays (for shallow depths on the terrace we use a penetration length of $\Lambda=160~{\rm g~cm}^{-2}$ appropriate for cosmic ray nucleons).

$$N_{i}(t) = N_{i}(0)e^{-\frac{(t+t_{2})/\tau_{i}}{2}} + \frac{P_{i}e^{-t_{2}/\tau_{i}}}{\left(\frac{1}{z} + \frac{\rho E}{\Lambda}\right)} \left[1 - e^{-\left(\frac{1}{z} + \frac{\rho E}{\Lambda}\right)t_{1}}\right] + N_{i,pb}$$
(3)

We assume steady erosion in the source area prior to burial. Following Granger (2014), to a close approximation we can write the relationship between N_{26} and N_{10} at the time of initial burial as shown in

equation (4).

$$\frac{N_{26}(0)}{N_{10}(0)} \approx \frac{(P_{26}/P_{10})}{1 + \frac{N_{10}}{P_{10}r_{10}}} \tag{4}$$

Equations (3) and (4) can be solved together with equation (2), but the solution requires knowledge of the erosion rate on the terrace, which may be variable for each individual clast. We therefore do not expect all samples to lie on a single curve in 26 Al $^{-10}$ Be space, as in the traditional isochron burial dating.

Fortunately, we can place some bounds on the burial age by considering the endmember cases of slow vs. rapid terrace erosion. For

Table 1
Cosmogenic sample information. All samples were obtained from square DD1 (see Fig. 4). The upper nine comprise non-artifactual samples whereas the lower four are Earlier Stone Age lithics. See Suppl. Fig. 2 for images of the samples.

Sample/Spatial ID	Weight (g)	Length (mm)	Lithic artifact	Sample type	Spit depth (cm)
3584/1203	-	71.7	No	Cobble fragment	220–225
3593/1212	_	51.5	No	Pebble	220-225
3596/1215	_	76.1	No	Cobble fragment	220-225
3732/1236	_	56.5	No	Split pebble	225-230
3733/1237	_	89.8	No	Split cobble	225-230
3746/1250	_	138.1	No	Cobble	225-230
3831/1258	_	95.5	No	Split cobble	230-235
3880/-	_	63.5	No	Pebble	230-235
3965/1309	_	123.8	No	Clast	235-240
3463/1132	250.8	101.2	Yes	Flake fragment	215-220
3724/1228	274.7	96.9	Yes	Incomplete flake	225-230
3727/1231	157.7	91.4	Yes	Incomplete flake	225-230
3857/1284	95.1	88.7	Yes	Incomplete flake	230–235

very slow terrace erosion ($\rho E/\Lambda < <1/\tau$) cosmogenic nuclide production on the terrace dominates, and solution of equations (3) and (4) approaches an endmember case similar to that for a single burial age of time t_2 . Conceptually, this is because the clast is never deeply buried on the terrace, and experiences continuous exposure. Alternatively, for very fast terrace erosion rates ($\rho E/\Lambda > 1/\tau$), the clast spends most of its time buried, and the solution approaches an endmember case equivalent to a single burial age of time t_1+t_2 , but offset from the origin. All samples should therefore be approximately bounded by two curves whose slopes represent a minimum burial age equivalent to the age of the youngest deposit, and a maximum age equivalent to the age of the oldest deposit (see Suppl. Fig. 3).

To date the Penhill Farm site, quartz was cleaned and processed following the procedures outlined in Kuman et al. (2021). The quartz samples were crushed, sieved to 0.25-0.50 mm, and cleaned by repeated selective dissolution in hot agitated 1% HF/HNO₃. Purified quartz was dissolved in 5:1 HF:HNO3 and spiked with beryllium carrier made in house. After dissolution, an aliquot was taken and the aluminum concentration determined by inductively-coupled plasma-optical-emission spectrometry (ICP-OES), and assigned an uncertainty of 2%. Sulfuric acid was added to the remaining sample, which was then evaporated to fumes to remove fluorides. The sample was taken to pH 14 and centrifuged to remove iron, titanium, and other elements. Amphoteric Al and Be remained in solution, and were precipitated at pH 7, rinsed, and dissolved in 0.4 M oxalic acid. Al and Be were separated by ion exchange chromatography in 0.4 M oxalic acid. Aluminum was then taken to dryness as the chloride and beryllium as nitrate after precipitation in the presence of EDTA. Both were decomposed to oxide by flame and mixed with niobium for measurement of isotope ratios by accelerator mass spectrometry (AMS) against standards KNSTD (Nishiizumi (2004) and KNSTD07 (Nishiizumi et al., 2007). All uncertainties are reported at one sigma. Local production rates were calculated following the approach in Kuman et al. (2021), where the average and standard deviation over the past two million years determined from Lifton et al. (2014) were applied $(P_{10} = 3.43 \pm 0.36 \text{ at g}^{-1}\text{yr}^{-1})$; we assumed $P_{26}/P_{10} = 6.8$. For the relatively shallow burial depth of ca. 2.5-4.0 m in sand of density 1.8 g cm⁻³, we assume a post-burial production rate ratio of 8.0, estimated using production rates by muons from Balco (2017), and production rates by nucleons having an attenuation length of 160 g cm⁻².

4. Results

The cosmogenic nuclide concentrations are provided in Table 2 and plotted in Fig. 5. It is evident from Fig. 5 that the data exhibit significant scatter about the best-fit isochron, as expected for a multiple-burial scenario. The best-fit age is 0.76 \pm 0.05 Ma, with an apparently high degree of precision, but the mean square weighted deviation (MSWD) is very large, at 16.6, indicating that the data do not fit the model. In addition, the intercept of the isochron is negative, which is an

unphysical solution to equations (1) and (2) and indicates that at least some of the samples are likely reworked from older, previously buried deposits and arrived at the site with depressed ²⁶Al/¹⁰Be ratios. Both the high MSWD and the negative intercept indicate that the isochron age cannot be considered reliable.

Is it possible to interpret the depositional histories of these clasts even if they do not conform to a well-behaved isochron? As explained in the methods section, above, we expect that the samples should be bounded by isochrons corresponding to the ages of the youngest and oldest deposit.

The age of the debris flow that deposited the sediment can be estimated based on the upper envelope of the data. Ideally, multiple samples would lie upon an envelope that forms a reasonable isochron. At Penhill Farm, five of the data points conform to an isochron with a burial age of 0.63 ± 0.08 Ma and an MSWD of 0.82, representing the age of the debris flow deposit. The remaining seven samples, including all of the artifacts, lie below this upper envelope and so have a longer history that must include multiple episodes of burial. Of these remaining seven samples, five lie on an isochron corresponding to a burial age of 1.12 ± 0.07 Ma with an MSWD of 0.24. We suggest that the grouping of these five samples, including three of the artifacts, indicates that they share a common history including a second burial episode, older than the age of the debris flow but far younger than the age of the upper terrace (~ 3.2 Ma). We believe that this most likely represents the age of the colluvial wedge deposit that was the source of the debris flow.

We therefore propose a possible interpretation of this scattered isochron diagram. The youngest ages indicate that the debris flow from which the samples were collected occurred near ca. 0.6 Ma, the age of the deposit. The debris flow would have been sourced from the nearby colluvial wedge uphill, from an area of the deposit that accumulated at ca. 1.1 Ma, as indicated by the isochron fit to five of the oldest samples (excluding one older clast). The debris flow would have deposited clasts with a range of burial histories, depending on their depth in the source area colluvium. Clasts near the surface of the colluvial source area would have a long exposure time and would have a burial age corresponding to the age of the debris flow (ca. 0.6 Ma), while well-shielded clasts from deep within the colluvial deposit would have an age corresponding to accumulation of the colluvial wedge in the source area (ca. 1.1 Ma). This scenario would explain the high degree of scatter and the full range of apparent burial ages observed on the isochron diagram. The observation that three out of the four artifacts have an apparent burial age of ca. 1.1 Ma suggests that the artifacts were buried in the colluvial source area at that time, and that hominins were present on the landscape while the colluvium was accumulating.

5. Discussion and conclusions

The new cosmogenic dating results in this study differ considerably from the original Terrace 9 burial age of 1.37 \pm 0.16 Ma (Granger et al.,

Table 2
Cosmogenic nuclide data.

Sample	Quartz mass	Be spike	Quartz [Al]	¹⁰ Be/ ⁹ Be	26 Al/ 27 Al	[¹⁰ Be]	[²⁶ Al]
	(g)	(10^{-6} g)	$(10^{-6} \text{g g}^{-1})$	$(x\ 10^{-15})$	$(x\ 10^{-15})$	$(10^3 {\rm at g}^{-1})$	(10^3 at g^{-1})
3584	22.303	266.1	193.8 ± 3.9	874.1 ± 19.4	740.5 ± 21.8	696.4 ± 15.4	3200 ± 114
3593	16.506	267.3	216.5 ± 4.3	452.6 ± 8.5	304.0 ± 11.7	488.7 ± 9.2	1468 ± 64
3596	42.744	268.1	172.3 ± 3.4	1548.7 ± 22.2	811.8 ± 23.2	649.2 ± 9.3	3120 ± 109
3732	34.255	268.1	89.5 ± 1.8	1143.4 ± 21.6	1346.1 ± 34.9	597.8 ± 11.3	2686 ± 88
3733	24.194	269.1	150.1 ± 3.0	608.7 ± 12.4	527.8 ± 16.3	451.8 ± 9.2	1767 ± 65
3831	37.121	269.0	99.3 ± 2.0	1105.3 ± 20.5	921.5 ± 25.4	535.1 ± 9.9	2040 ± 70
3880	28.755	268.5	120.9 ± 2.4	413.5 ± 9.4	445.6 ± 13.9	257.3 ± 5.8	1202 ± 45
3965	39.948	269.0	95.2 ± 1.9	1788.4 ± 32.0	1797.9 ± 44.3	805.0 ± 14.4	3818 ± 121
3463	28.631	275.7	239.2 ± 4.8	1666.0 ± 24.2	680.4 ± 18.7	1072.4 ± 15.6	3630 ± 100
3724	25.043	275.6	85.4 ± 1.7	218.6 ± 8.5	418.3 ± 14.9	159.7 ± 6.2	721 ± 26
3727	33.562	275.7	182.8 ± 3.7	1090.0 ± 18.4	533.7 ± 11.3	598.2 ± 10.1	2176 ± 46
3857	6.782	275.3	252.3 ± 5.0	154.6 ± 10.5	274.5 ± 17.6	415.4 ± 28.2	1545 ± 99
Blank	-	266.4	2080 μg	1.64 ± 0.52	1.65 ± 0.75		

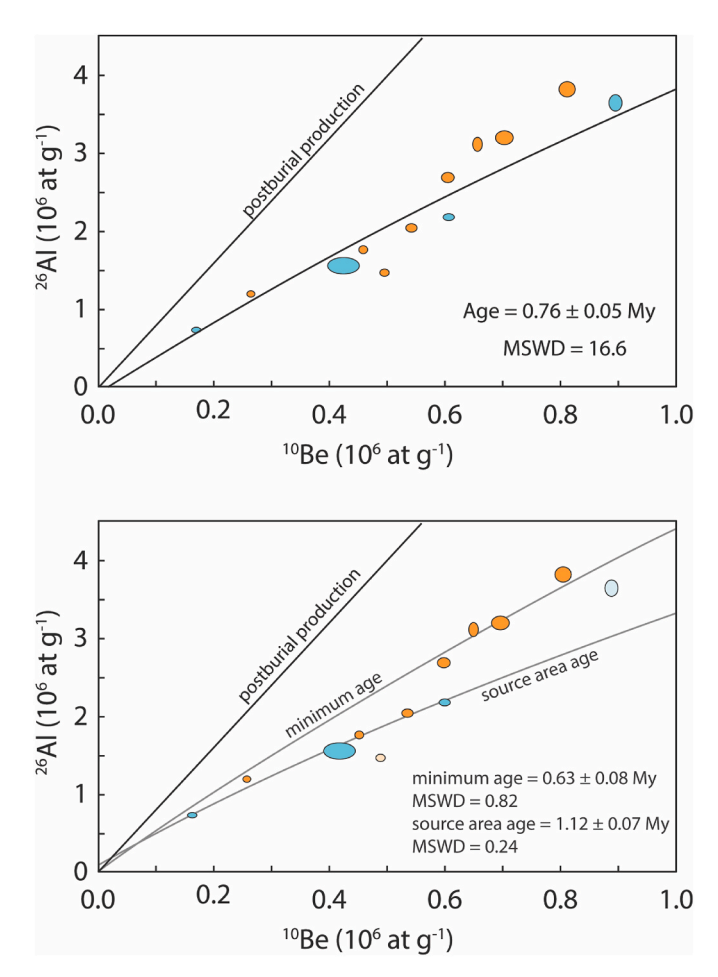


Fig. 5. Burial isochrons for the Penhill Farm samples. Data points are shown as $1\text{-}\sigma$ error ellipses. Artifacts are shown in blue, and non-artifactual quartz shown in orange. Upper graph shows best-fit isochron to all data points. The high MSWD indicates a poor fit to the data. Lower graph shows two bounding isochrons constraining the range of ages. The minimum age corresponds to an upper envelope and indicates the timing of the debris flow, while the source area age represents the timing of sediment accumulation in the colluvial source area. Two samples not fit to either curve are shown in light colors.

2013). This is consistent with stratigraphy; because the deposit is a debris flow in a channel developed within the top of the terrace, it must be younger than the terrace itself.

The contextual nature of the archaeological deposit in the debris flow, together with abundant calcrete and silcrete nodules, are consistent with the interpretation that the artifacts were not deposited *in situ*,

but were reworked from a deposit upslope. The artifact assemblage at the site is extremely well-preserved, with more than 75% of the stone tools being fresh and unabraded, with sharp edges. This is consistent with the artifacts having been protected from erosion by being buried in a colluvial deposit prior to deposition in the debris flow, as we have proposed here. Prior burial is further supported by the high retention of the smallest assemblage components (fragments <20 mm exceed 50%; Lotter 2016) in the debris flow, which argues against extensive assemblage winnowing during exposure at the ground surface.

The isochron burial dating method as defined by equations (1) and (2) assumes that all samples are deposited simultaneously, and that they were derived from an eroding landscape with little sediment storage. This method works well in many settings, including alluvial terraces and cave deposits. As we have shown here, however, debris flow deposits do not necessarily conform to the conditions for a reliable isochron. In this case, the ²⁶Al and ¹⁰Be together indicate a range of burial ages rather than a single depositional age, because the clasts are derived from mobilization of an older colluvial deposit. We have shown here, however, that a reasonable interpretation of the data can be made, in which an envelope defining the youngest bounding isochron indicates the time of debris flow deposition, while an isochron formed by older samples within the dataset indicates the time of deposition of the debris flow source deposit.

Our interpretation of a two-stage history indicates that artifacts at Penhill Farm date to approximately 1.1 Ma, providing a better understanding of the age of the technology preserved at Penhill Farm. Our new age estimate confirms the antiquity of the regional occupations by stone-tool-making hominins during the Early Pleistocene. The results from Penhill Farm also support observations of Acheulean artifacts from elsewhere in the Sundays River Valley – at the other dated Terrace 9 site called Bernol Farm with an age of 1.14 \pm 0.2 Ma – confirming that regional occupations began at least ca. 1 Ma.

From our descriptions of the archaeology, we know that the ancestors of early modern humans were already in this area well before the technological advancements that typify the regional MSA sequence, and collectively the Sundays River sites therefore provide insightful detail on the artifact production strategies that hominins employed while subsisting on the local paleo-landscape. Some comparison can be made between the Penhill and Bernol Farm artifacts (Lotter and Kuman 2018b) in this regard, particularly for the large cutting tools (LCTs, namely handaxes, cleavers, picks and bifaces). Although the sample of LCTs from Bernol Farm is small (n = 11, versus n = 49 for Penhill), both sites confirm that the production of tools with predominantly convergent – albeit generalized – tip shapes on large flake blanks was favored, and these tips may have been useful in a wide variety of on-site tasks (Lotter and Kuman 2018b; Lotter 2020a). Shaping strategies also predominantly employ bifacial flaking (flakes removed from both LCT surfaces), but tool elongation (length/width) and refinement (thickness/width) ratios indicate that the Penhill tools retain longer lengths

and thinner profiles than those sampled at Bernol. However, this is coupled with less extensive shaping (as reflected by the quantity of flake scars and percentage of remaining cortex – unmodified outer rock surface). Collectively, these patterns suggest that tool blank properties played an important role in overall LCT forms in the Sundays Valley, as hominins at Penhill Farm were able to source higher quality flake blanks that were relatively longer and provided thinner profiles prior to tool shaping, thus negating the need for extensive reduction.

There is also an over-representation of large tools and flakes at Penhill Farm relative to the associated core sample (Lotter and Caruana 2021; also see Lotter 2022), and it appears that hominins sourced these larger, better-quality flakes from large cores off-site. At Bernol Farm we have direct evidence for such activity whereby large boulder cores occur on-site. This would suggest that hominins at the two sites employed different tool blank sourcing strategies. At Penhill Farm, they intentionally sourced and transported materials from the upper terrace nearby for production at a later stage (Lotter and Caruana 2021; also see discussion by Mesfin et al., 2021 for detail on these local clast selection strategies), while at Bernol Farm the hominins appeared to focus their acquisition strategies more locally on large clasts obtained closer to the river channel or in older higher terraces nearby (Lotter and Kuman 2018b). These strategies may reflect differences in behavior, or alternatively they may reflect the different geomorphic settings in which the artifacts were found, with the Penhill artifacts recovered from a setting further from the active river channel. In both cases, however, these secondary context Acheulean assemblages show that hominins were utilizing the riparian landscape by ca. 1 Ma. Collectively, the Sundays River sites aid our understanding of the local archaeological sequence, and the dating results presented here will further facilitate their inclusion into the southern African ESA chronology.

Declaration of competing interest

The authors declare that they have no known competing financial interests or personal relationships that could have appeared to influence the work reported in this paper.

Data availability

Data will be made available on request.

Acknowledgments

The Palaeontological Scientific Trust (PAST), Johannesburg, South Africa, provided funds for the direct dating of artifacts, as well as bursary support to MGL. This research was also supported by the National Research Foundation (NRF), the University of Johannesburg (URC Senior Postdoctoral Research Fellowship awarded to MGL), and the Palaeo-Research Institute (P-RI). The authors wish to thank Errol and Lindi Hewson, formerly of Penhill Farm, for their support and assistance. The authors also wish to thank N. Phillips, R. Couzens and H. Li for assistance in the field.

Appendix A. Supplementary data

Supplementary data to this article can be found online at https://doi.org/10.1016/j.quageo.2023.101431.

References

Balco, G., 2017. Production rate calculations for cosmic-ray-muon-produced ¹⁰Be and ²⁶Al benchmarked against geological calibration. Quat. Geochronol. 39, 150–173. Caruana, M.V., Lotter, M.G., 2022. Comparing morphological variability in handaxes from Penhill farm and Amanzi Springs, eastern Cape, South Africa. Southern African Field Archaeology 17, 1246.

- Chmeleff, J., von Blanckenburg, F., Kossert, K., Jakob, D., 2010. Determination of the ¹⁰Be half-life by multicollector ICP-MS and liquid scintillation counting. Nucl. Instrum. Methods Phys. Res., Sect. B 268, 192–199.
- Council for Scientific and Industrial Research (CSIR), 2011. NFEPA rivers vector geospatial dataset. Viewed September 2020 at. http://bgis.sanbi.org/SpatialDataset/Detail/397.
- d'Errico, F., Stringer, C.B., 2011. Evolution, revolution or saltation scenario for the emergence of modern human cultures? Philo. Trans. Royal Soc. B 366, 1060–1069.
- Davies, O., 1971. Pleistocene shorelines in the southern and south-eastern Cape Province (Part 1). Ann. Natal. Mus. 21, 183–223.
- Davies, O., 1972. Pleistocene shorelines in the southern and south-eastern Cape Province (Part 2). Ann. Natal. Mus. 21, 225–279.
- Deacon, H.J., 1970. The acheulean occupation at Amanzi Springs uitenhage district, Cape Province. Annals Cape Pro. Museums 8, 89–189.
- Dollar, E.S.J., 1998. Palaeofluvial geomorphology in southern Africa: a review. Prog. Phys. Geogr. 22, 325–349.
- Erlanger, E.D., 2010. Rock Uplift, Erosion, and Tectonic Uplift of South Africa
 Determined with Cosmogenic ²⁶Al and ¹⁰Be. Unpublished MSc dissertation, Indiana
 (Purdue University).
- Erlanger, E.D., Granger, D.E., Gibbon, R.J., 2012. Rock uplift rates in South Africa from isochron burial dating of fluvial and marine terraces. Geology 40, 1019–1022.
- Granger, D.E., 2014. Cosmogenic nuclide burial dating in archaeology and paleoanthropology. In: Holland, H.D., Turekian, K.K. (Eds.), Treatise on Geochemistry, second ed., Volume 14. Elsevier, Oxford, pp. 81–97.
- Granger, D.E., Gibbon, R.J., Kuman, K., Lotter, M.G., Erlanger, E., 2013. Isochron Burial dating method and application to an earlier stone age chronosequence on the Sundays River, South Africa. In: Poster presented at the Association of Southern African Professional Archaeologists Biennial Conference. Gaborone, Botswana.
- Hattingh, J., 1994. Depositional environment of some gravel terraces in the Sundays River Valley, eastern Cape. S. Afr. J. Geol. 97, 156–166.
- Hattingh, J., 1996. Fluvial response to allocyclic influences during the development of the lower Sundays River, Eastern Cape, South Africa. Quat. Int. 33, 3–10.
- Hattingh, J., 2008. Fluvial systems and landscape evolution. In: Lewis, C.A. (Ed.), Geomorphology of the Eastern Cape: 21-42. Grahamstown (NISC)
- Hattingh, J., Goedhart, M.L., 1997. Neotectonic control on drainage evolution in the Algoa Basin, southeastern Cape Province, S. Afr. J. Geol. 100, 43–52.
- Hattingh, J., Rust, I.C., 1999. Drainage evolution of the Sundays River, South Africa. In: Miller, A., Gupta, A. (Eds.), Varieties in Fluvial Form: 145-166. John Wiley and Sons, Chichester.
- Haughton, S.H., 1928. The Geology of the Country between Grahamstown and Port Elizabeth: an Explanation of Cape Sheet No. 9 (Port Elizabeth). Geological Survey of South Africa.
- Henshilwood, C.S., d'Errico, F., Yates, R., Jacobs, Z., Tribolo, C., Duller, G.A.T., Mercier, N., Sealy, J.C., Valladas, H., Watts, I., Wintle, A.G., 2002. Emergence of modern human behavior: middle Stone Age engravings from South Africa. Science 295, 1278–1280.
- Henshilwood, C.S., d'Errico, F., Vanhaeren, M., van Niekerk, K., Jacobs, Z., 2004. Middle stone age shell beads from South Africa. Science 304, 404.
- Inskeep, R.R., 1965. Earlier stone age occupation at Amanzi: a preliminary investigation. South Afr. J. Sci. 61, 229–242.
- Korschinek, G., Bergmaier, A., Faestermann, T., Gerstmann, U.C., Knie, K., Rugel, G., Wallner, A., Dillmann, I., Dollinger, G., Von Gostomski, C.L., Kossert, K., 2010. A new value for the half-life of ¹⁰Be by heavy-ion elastic recoil detection and liquid scintillation counting. Nucl. Instrum. Methods Phys. Res., Sect. B 268, 187–191.
- Kuman, K., Granger, D.E., Gibbon, R.J., Pickering, T.R., Caruana, M.V., Bruxelles, L., Clarke, R.J., Heaton, J.L., Stratford, D., Brain, C.K., 2021. A new absolute date from Swartkrans Cave for the oldest occurrences of *Paranthropus robustus* and Oldowan stone tools in South Africa. Journal of Human Evolution 156, 103000.
- Kuman, K., Lotter, M.G., Leader, G.M., 2020. The Fauresmith of South Africa: a new assemblage from Canteen Kopje and significance of the technology in human and cultural evolution. J. Hum. Evol. 148, 102884.
- Laidler, P.W., 1947. The evolution of middle palaeolithic technique at geelhout, near kareedouw, in the southern Cape. Trans. Roy. Soc. S. Afr. 31, 283–313.
- Lifton, N., Sato, T., Dunai, T.J., 2014. Scaling in situ cosmogenic nuclide production rates using analytical approximations to atmospheric cosmic-ray fluxes. Earth Planet Sci. Lett. 386, 149–160.
- Lombard, M., Wadley, L., Deacon, J., Wurz, S., Parsons, I., Mohapi, M., Swart, J., Mitchell, P., 2012. South African and Lesotho Stone Age sequence updated (I). S. Afr. Archaeol. Bull. 67, 120–144.
- Lotter, M.G., 2016. The archaeology of the lower Sundays River Valley, eastern Cape Province, South Africa: an assessment of earlier stone age alluvial terraces sites. In: Unpublished PhD Thesis. University of the Witwatersrand, Johannesburg.
- Lotter, M.G., 2020a. A preliminary assessment of large cutting tool production at the acheulean site of Penhill farm, lower Sundays River Valley, eastern Cape Province, South Africa. S. Afr. Archaeol. Bull. 75, 58–69.
- Lotter, M.G., 2020b. An introduction to the formal tools from the acheulean site of Penhill farm, lower Sundays River Valley, South Africa. S. Afr. Archaeol. Bull. 75, 146–155.
- Lotter, M.G., 2022. Final piece(s) of the puzzle: the remaining artefacts at Penhill Farm, South Africa, and their significance for understanding lithic production. S. Afr. Archaeol. Bull. 77, 140–153.
- Lotter, M.G. in press The lower Sundays River Valley: Atmar, Bernol and Penhill Farms. In: Beyin, A., Wright, D.K., Wilkins, J., Bouzouggar, A. & Olszewki, D.I. (eds) Handbook of Pleistocene Archaeology of Africa: Hominin Behaviour, Geography, and Chronology. Springer Nature, Switzerland.

- Lotter, M.G., Caruana, M.V., 2021. Exploring core reduction preferences at Penhill farm, lower Sundays River Valley, South Africa. S. Afr. Archaeol. Bull. 76, 140–150.
- Lotter, M.G., Kuman, K., 2018a. The acheulean in South Africa, with announcement of a new site (Penhill farm) in the lower Sundays River Valley, eastern Cape Province, South Africa. Quat. Int. 480, 43–65.
- Lotter, M.G., Kuman, K., 2018b. Atmar and Bernol farms: new acheulean sites in the lower Sundays River Valley, eastern Cape Province, South Africa. S. Afr. Archaeol. Bull. 73, 64–74.
- Marean, C., 2010. Pinnacle Point Cave 13B (Western Cape Province, South Africa) in context: the Cape floral kingdom, shellfish, and modern human origins. J. Hum. Evol. 59, 425-443.
- McBrearty, S., Brooks, A.S., 2000. The revolution that wasn't: a new interpretation of the origin of modern human behavior. J. Hum. Evol. 39, 453–563.
- Mesfin, I., Lotter, M.G., Benjamim, M.H., 2021. A new approach to quantifying raw material selectivity in the African Acheulean: perspectives from Angola and South Africa. J. Afr. Archaeol. 19, 205–234.
- NASA JPL, 2013. NASA shuttle radar topography mission water body data shapefiles & raster files dataset (NASA EOSDIS land pro- cesses DAAC). https://doi.org/10.5067/MEaSUREs/SRTM/SRTMSWBD.003. Viewed September 2020 at.
- Nishiizumi, K., 2004. Preparation of ²⁶Al AMS standards. Nucl. Instrum. Methods Phys. Res., Sect. B 223, 388–392.

- Nishiizumi, K., Imamura, M., Caffee, M.W., Southon, J.R., Finkel, R.C., McAninch, J., 2007. Absolute calibration of ¹⁰Be AMS standards. Nucl. Instrum. Methods Phys. Res., Sect. B 258, 403–413.
- Ruddock, A., 1948. Terraces in the lower part of the Sundays River Valley, Cape Province. Trans. Roy. Soc. S. Afr. 31, 347–370.
- Ruddock, A., 1957. A note on the relation between chelles-acheul implements and quaternary river terraces in the valleys of the Coega and Sundays rivers, Cape Province. South Afr. J. Sci. 53, 373–377.
- Ruddock, A., 1968. Cenozoic sea-levels and diastrophism in a region bordering Algoa Bay. Trans. Geol. Soc. S. Afr. 71, 209–233.
- Wilkins, J., Chazan, M., 2012. Blade production ~500 thousand years ago at Kathu Pan 1, South Africa: support for a multiple origins hypothesis for early Middle Pleistocene blade technologies. J. Archaeol. Sci. 39, 1883–1900.
- Wurz, S., 2013. Technological trends in the middle stone age of South Africa between MIS 7 and MIS 3. Curr. Anthropol. 54, 305–319.
- Wurz, S., 2020. Southern and east african middle stone age: geography and culture. In: Smith, C. (Ed.), Enclyclopedia of Global Archaeology: 10048-10068. Springer, New York.
- Council for Geosciences (CGS), 2008. Simplified Geological Map of the Republic of South Africa and the Kingdoms of Lesotho and Swaziland, Compiled by Johnson. M.R. & Wolmarans, L.G. Pretoria, South Africa: CGS.